Electronic Research Archive

ERA, 31(1): 147–168.
DOI: 10.3934/era.2023008
Received: 04 August 2022
Revised: 20 September 2022
Accepted: 22 September 2022
Published: 26 October 2022

http://www.aimspress.com/journal/ERA

Research article

Nonlinear programming for fleet deployment, voyage planning and speed optimization in sustainable liner shipping

Yiwei Wu[1], Yadan Huang[2,*], H Wang[3,4,5] and Lu Zhen[6]

[1] Department of Logistics and Maritime Studies, The Hong Kong Polytechnic University, Hung Hom, Kowloon, Hong Kong

[2] Sino-US Global Logistics Institute, Antai College of Economics and Management, Shanghai Jiao Tong University, Shanghai 200030, China

[3] School of Mathematics and Applied Statistics, University of Wollongong, Wollongong, NSW 2522, Australia

[4] Strome College of Business, Old Dominion University, Norfolk, VA 23529, USA

[5] Faculty of Business, The Hong Kong Polytechnic University, Hung Hom, Kowloon, Hong Kong

[6] School of Management, Shanghai University, Shanghai 200436, China

* **Correspondence:** Email: yadan.huang@outlook.com; Tel: +8618816933968.

Abstract: Limiting carbon dioxide emissions is one of the main concerns of green shipping. As an important carbon intensity indicator, the Energy Efficiency Operational Index (EEOI) represents the energy efficiency level of each ship and can be used to guide the operations of ship fleets for liner companies. Few studies have investigated an integrated optimization problem of fleet deployment, voyage planning and speed optimization with consideration of the influences of sailing speed, displacement and voyage option on fuel consumption. To fill this research gap, this study formulates a nonlinear mixed-integer programming model capturing all these elements and subsequently proposes a tailored exact algorithm for this problem. Extensive numerical experiments are conducted to show the efficiency of the proposed algorithm. The largest numerical experiment, with 7 ship routes and 32 legs, can be solved to optimality in four minutes. Moreover, managerial insights are obtained according to sensitivity analyses with crucial parameters, including the weighting factor, unit price of fuel, Suez Canal toll fee per ship, weekly fixed operating cost and cargo load in each leg.

Keywords: fleet deployment optimization; EEOI; maritime decarbonization; voyage planning; carbon

dioxide emission

1. Introduction

Climate change is arguably one of the greatest challenges of our time. Although shipping is regarded as an environmentally efficient mode of transportation, it generates tremendous air emissions that have harmful effects on the global environment. Carbon dioxide (CO_2) accounts for the vast majority of greenhouse gas emissions from the transportation sector [1]. Moreover, United Kingdom broker Simpson Spence Young estimated that CO_2 emissions from global shipping in 2021 increased 4.9% from 2020 and surpassed 2019 levels [2]. Unless serious actions are taken soon, CO_2 emissions from global shipping may increase by between 50 and 250% by 2050 [3], which undoubtedly will contribute to global warming.

Maritime decarbonization in particular is necessary to achieve the long-term goal of the Paris Agreement adopted at the Paris climate conference (COP21) in 2015 [4], that is, to limit the increase in the average global temperature to well below 2 °C, preferably to 1.5 °C, above pre-industrial levels. For this reason, many emission limits and regulations are promulgated to reduce CO_2 emissions and stop global warming. For example, the International Maritime Organization (IMO), which is the United Nations specialized agency for international shipping, has set strategies to reduce carbon emissions per unit of transport work by at least 40% by 2030 and reduce the total annual greenhouse gas emissions from international shipping by at least 50% by 2050, with 2008 as a baseline [5]. Despite the intensifying regulatory environment, international shipping released 833 million tons of CO_2 in 2021, an increase of 4.9% from 2020 [6]. Hence, it is urgent for liner companies to consider how to reduce carbon emissions when scheduling shipping activities to meet international requirements.

The carbon emissions per unit of transport work can be referred to as the carbon intensity, and one of the carbon intensity indicators is the EEOI, which was introduced by the IMO in 2009 and enforced in 2011 to measure the energy efficiency level of each operating ship [7]. The EEOI value of a ship over a year reflects the energy efficiency of the ship and may help liner companies to schedule ship fleets when considering the maritime decarbonization target. The EEOI value of a ship can be calculated by dividing annual carbon emissions of the ship (g) by actual ton-miles carried by the ship (the amount of transported cargo times total travel distance) in the year [8]. Therefore, the EEOI value of a ship is directly influenced by the type of used fuel, cargo load and total distance traveled. The lower the EEOI value is, the better the energy efficiency performance. From an operational perspective, several operation decisions, such as voyage planning and speed optimization, which further influences fleet deployment, can be jointly optimized to reduce the EEOI because these decisions directly affect fuel consumption. Moreover, displacement (tons), i.e., the total weight of the ship itself, cargo, ballast water and bunker, also influences fuel consumption [9]. Hence, seeking the optimal fleet deployment, voyage planning and speed to achieve liner operations management optimization is an efficient way to reduce EEOI, achieve energy savings and reduce emissions.

This study is motivated by the abovementioned real-world challenge in green shipping, and it may contribute to liner operations management by proposing a nonlinear mixed-integer programming (MIP) model and a tailored exact algorithm. Two assumptions are considered in this study: 1) Ships are homogenous on each route in terms of the cost structure, which is consistent with the assumptions considered in Zhen et al. [10]; 2) ships' dwell time at all ports of call on a ship route is given, which is

in line with the assumptions considered in Zhen et al. [11]. This study provides liner companies with scientific methods to optimize fleet deployment, voyage planning and speed to reduce both the total weekly cost and the average EEOI value of all deployed ships on all routes with the consideration of the influences of sailing speed, displacement and voyage option on fuel consumption. Eleven sets of numerical experiments with different route compositions were first conducted to evaluate the performance of the proposed algorithm. Moreover, sensitivity analyses with crucial parameters, including the weighting factor, unit price of fuel, Suez Canal toll fee per ship, weekly fixed operating cost and cargo load in each leg, are carried out to show the influence of these aspects on the results to look for managerial insights.

The remainder of this study is organized as follows. Related works are reviewed in Section 2. Section 3 elaborates on the problem background and proposes a nonlinear MIP model for the integrated problem. A tailored exact algorithm is designed in Section 4. Section 5 reports the computational experiments, including basic experiments to evaluate the efficiency of the proposed algorithm and sensitivity analyses to seek managerial insights. Conclusions are outlined in the last section.

2. Literature review and discussion

The core part of this study is related to the widely-studied fleet deployment problem. Readers interested in overviews of the above problem can refer to Meng et al. [12], Wang and Meng [13] and Christiansen et al. [14]. This study focuses on an integrated optimization problem of fleet deployment, voyage planning and speed optimization to minimize both the total weekly cost and the average EEOI value of all deployed ships on all routes. Thus, this section reviews the streams of related literature from the following two perspectives: the fleet deployment problem and studies related to EEOI.

The first research stream is concerned with the fleet deployment problem. As an important concern for liner companies, the fleet deployment problem determines the number of ships to be deployed on various ship routes to maximize the total profit or to minimize the total cost. Lai et al. [15] formulated a two-stage model for a fleet deployment problem with shipping revenue management under demand uncertainty whose randomness is represented by probability-free uncertain sets. They also developed a column-and-constraint generation based exact algorithm to solve the model. In recent years, sustainable development is the main development direction of the shipping industry [16]. One of the most important green shipping factors in the fleet deployment problem is reducing emissions from ships, such as CO_2, sulfur oxides (SO_X) and nitrogen oxides (NO_X). Zhu et al. [17] investigated the influence of a maritime emissions trading system on fleet deployment and mitigation of CO_2 emissions. They proposed a stochastic integer programming model to determine fleet deployment and CO_2 emissions with different CO_2 prices. Considering sulfur emission control areas, Wang et al. [18] studied an integrated problem of schedule design, fleet deployment, sailing optimization and path selection, and they proposed a nesting algorithmic framework to solve the problem. Pasha et al. [19] designed a decomposition-based heuristic algorithm to solve an integrated problem of service frequency determination, fleet deployment, speed optimization and ship schedule design considering emissions released by ships with the aim of maximizing the total turnaround profit. Zhao et al. [20] formulated a two-stage stochastic linear model for a fleet renewal problem considering three sulfur reduction technologies and uncertain markets. With the consideration of sulfur emission limits, Chen et al. [21] built an ellipsoidal uncertainty set to describe demand uncertainties and developed a robust optimization model for an alliance fleet deployment problem with slot exchange. Moreover, Zhao et

al. [22] investigated how to reduce SO_X and NO_X emissions in shipping economically by determining the optimal technology choice.

The second topic considered in the related works is EEOI. Operational data, such as speed and deadweight, are usually used to analyze EEOI. Existing papers on EEOI mainly focus on two aspects, namely, estimation of EEOI values and scheduling based on EEOI values. In terms of the estimation of EEOI values, Acomi and Acomi [23] used commercial software to estimate the value of EEOI before a voyage, and they compared estimated values and true values according to speeds, days on anchor and waiting days. In terms of scheduling based on EEOI values, Hou et al. [24] formulated a sailing speed optimization model with consideration of uncertain ice loads to minimize the EEOI value of each ship in ice areas. Sun et al. [25] developed a dynamic optimization model for sailing speeds of ships to improve fuel efficiency as well as reduce EEOI. They used a neural network to predict fuel consumption rate and ship speed, and they applied a genetic algorithm to optimize engine revolution and seek the minimum EEOI. Considering the uncertainty in ice loads as well as water velocity, Ichsan et al. [26] studied a decided route on the sea tollway of Indonesia and optimized the rate of EEOI of ships deployed on the route. With the aim of minimizing EEOI values of seven types of specialized ships, Prill et al. [27] assumed that the EEOI of each ship is related to the deadweight of the ship, the type and amount of consumed fuel and the voyage distance traveled by the ship, and they proposed a new method of determining the EEOI of each ship by optimizing sailing speeds of ships and the realization time of each exploitation task. Hou et al. [28] developed a ship speed optimization model which brought a 15% reduction in EEOI in the computational experiment.

In summary, the prevailing trend in the fleet deployment problem is studying how to reduce emissions from the shipping industry because of the increasing public concern about environmental protection. However, few works focus on an integrated optimization problem of fleet deployment, voyage planning and speed optimization to minimize both the total weekly cost and the average EEOI value of all deployed ships on all routes. Therefore, this paper studies an integrated optimization problem of fleet deployment, voyage planning and speed optimization with consideration of the influences of sailing speed, displacement and voyage option on fuel consumption. Moreover, some other frequently ignored operating limits, such as Suez Canal toll fee, are considered in this paper. This study proposes a nonlinear MIP model to minimize two objectives, i.e., the total weekly cost and the average EEOI value of all deployed ships on all routes, by determining the optimal fleet deployment, voyage planning and speed.

3. Problem description and model formulation

This study is oriented toward an integrated optimization problem of fleet deployment, voyage planning and speed optimization with consideration of the influences of sailing speed, displacement and voyage option on fuel consumption. This section first elaborates on the detailed background of the problem in Section 3.1, explains the objective function of the problem in Section 3.2 and presents the mathematical model in Section 3.3.

3.1. Problem background

We consider a liner company operating on a network containing a set R of container ship routes (services). The liner company has already determined the optimal service plan including fleet

deployment, sailing speed and voyage selection. However, in the context of the Carbon Intensity Indicator (CII) introduced by the IMO, especially considering EEOI, the liner company may need to reoptimize their service plan including fleet deployment, sailing speed and voyage options such as the Cape of Good Hope route or the Suez Canal route [29] in Figure 1.

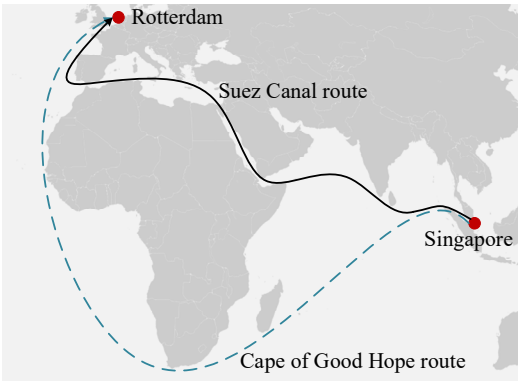

Figure 1. Comparison of two voyage options: Suez Canal route and Cape of Good Hope route.

Some ship routes, e.g., r $(r \in R)$, operated by the liner company may contain the voyage between Asian ports and European ports. We assume that the liner company originally selects the Suez Canal route for these voyages because sailing through the Suez Canal saves a lot of time. In this case, let I_r and I_r' represent the set of legs that do not cross Asian and European ports on ship route r and the set of legs across Asian and European ports on ship route r, respectively. For example, Table 1 summarizes the sets of I_r and I_r' of route r whose port rotation is Qingdao-Shanghai-Ningbo-Yantian-Rotterdam-Hamburg-Antwerp-Singapore-Qingdao. We then let γ_{ri} denote a binary variable which equals 1 if and only if the voyage option of leg i, $i \in I_r'$, on ship route r selects the Suez Canal voyage and equals 0 if selecting the Cape of Good Hope voyage. In addition, sailing speeds of deployed ships during each leg should be between $\underline{v}$ and $\overline{v}$, where $\underline{v}$ and $\overline{v}$ represent the minimum and maximum speeds of ships on ship routes, respectively. Let V represent a set of all possible sailing speeds indexed by v, and $V = \{\underline{v}, \underline{v} + 0.1, \ldots, \overline{v} - 0.1, \overline{v}\}$.

Table 1. Summary of sets I_r and I_r'.

Set	Leg		
I_r	Qingdao → Shanghai	Shanghai → Ningbo	Ningbo → Yantian
	Rotterdam → Hamburg	Hamburg → Antwerp	Singapore → Qingdao
I_r'	Yantian → Rotterdam	Antwerp → Singapore	

In terms of fleet deployment and speed optimization, EEOI values of all deployed ships on all ship routes should be regarded as an important consideration because when stricter CO_2 emission reduction regulations issued by international organizations take effect, liner companies have to find ways to reduce their deployed ships' EEOI values. The incorporation of EEOI may result in higher costs for liner companies in practice; however, companies certainly aim to minimize their total cost while complying with EEOI regulations. Therefore, this study considers the influences of sailing speed, displacement and voyage option on fuel consumption. Bi-objective programming has been widely applied before when minimizing carbon emissions and maximizing profit of liner companies, such as

in Zhao et al. [30]. From the perspective of the liner company, this study develops a bi-objective model to balance the total weekly cost, including the weekly fixed operating cost, weekly Suez Canal toll fee and weekly fuel cost, and the average EEOI value of all deployed ships on all ship routes by determining fleet deployment, voyage planning and sailing speed of all deployed ships. The above strategic-level problem involves many intertwined decisions, so a scientific decision-making methodology is needed for this problem.

3.2. Objective function

This problem is formulated as a bi-objective programming model. These two objective functions are the total weekly cost and the average EEOI value of all deployed ships on all routes. In the following paragraphs, we first explain separately how to formulate these two objective functions and then introduce how to deal with the bi-objective programming.

The first objective function focuses on the total weekly cost, which contains three parts: the weekly fixed operating cost, weekly Suez Canal toll fee and weekly fuel cost. Specifically, the first part is the weekly fixed operating cost of deployed ships. Because a fleet of homogeneous ships is deployed on each route to maintain a weekly service frequency, the total fixed operating cost for all deployed ships on all routes during one week can be calculated as $\sum_{r\in R} o\beta_r$, where o and β_r denote the weekly operating cost for deploying one ship on ship routes and the number of ships deployed on route r, respectively. Next is the weekly Suez Canal toll fee faced by the liner company. Let q_r denote the Suez Canal toll fee of each ship deployed on route r (USD/ship). Hence, we can calculate the weekly Suez Canal toll fee by $\sum_{r\in R}\sum_{i\in I_r'} q_r\gamma_{ri}$.

The last part of the total weekly cost is the fuel cost, which depends on fuel consumption. Each ship contains a main engine, which provides propulsion power for the ship, and an auxiliary engine, which provides power for uses other than propulsion. Specifically, in terms of fuel consumption of the main engine, most of the existing fuel consumption models in the literature [11,31,32] agreed that a ship's unit fuel consumption significantly depends on its sailing speed and calculated the unit fuel consumption function by $\dot{c}v^{\ddot{c}}$ to conduct liner shipping network analyses, where v is sailing speed (knots), and $\dot{c}$ and $\ddot{c}$ are positive coefficients. However, apart from sailing speed, several other factors also influence fuel consumption. The first one is displacement (tons), i.e., the total weight of the ship itself, cargo, ballast water and bunker. Meng et al. [9] investigated the relationship between the fuel consumption rate of a container ship and several factors, including sailing speed, displacement and weather/sea conditions. However, it is extremely difficult to record the precise weather/sea conditions because the effects of waves, wind and currents are interwoven in practice. Hence, the influence of weather/sea conditions on fuel consumption is not considered in this study. Also, this study formulates the unit fuel consumption function as $c_1v^{c_2}d^{c_3}$ (tons/hour), which is given by Meng et al. (2016) [9], where c_1, c_2 and c_3 are positive coefficients, and v and d represent the actual sailing speed (knots) and displacement (tons) of the ship during one leg, respectively. Finally, in terms of fuel consumption of the auxiliary engine, we assume the auxiliary engine of a ship deployed on ship route r consumes an amount e_r of fuel per day. In summary, the total amount of fuel consumed by a ship's main engine on ship route r, denoted by ε_r, can be calculated by $\varepsilon_r = \sum_{i\in I_r}\sum_{v\in V} c_1v^{c_2}\alpha_{riv}{d_{ri}}^{c_3}\frac{l_{ri}}{v} + \sum_{i\in I_r'}\sum_{v\in V} c_1v^{c_2}\alpha_{riv}{d_{ri}}^{c_3}\frac{l_{ri}\gamma_{ri}+l_{ri}'(1-\gamma_{ri})}{v}$, where α_{riv}, d_{ri}, l_{ri} and

l'_{ri} represent, respectively, a binary variable which equals 1 if and only if the speed of the ship sailing during leg i on route r is v and 0 otherwise, actual displacement (tons) of the ship during leg i on ship route r, length (n mile) of the ith leg if $i \in I_r$ or length of the ith leg taking the Suez Canal route if $i \in I'_r$ on ship route r and length (n mile) of the ith ($i \in I'_r$) leg taking the Cape of Good Hope route on ship route r. Weekly fuel consumption of auxiliary engines of all deployed ships on route r is $7e_r\beta_r$ because the total time for a ship completing travel along route r including dwell time and sailing time is $7\beta_r$ days to maintain a weekly container shipping service frequency. In summary, the total weekly fuel cost of all deployed ships on all routes is $\sum_{r\in R}(a_1\varepsilon_r + 7a_2e_r\beta_r)$, where a_1 and a_2 are the unit prices of fuels consumed by the main and auxiliary engines, respectively (USD/ton). Therefore, the total weekly cost can be calculated by $\sum_{r\in R}[o\beta_r + \sum_{i\in I'_r} q_r\gamma_{ri} + a_1\varepsilon_r + 7a_2e_r\beta_r]$.

The second objective is the average EEOI value of all deployed ships on all routes. According to the IMO [8], the EEOI of a ship is described by the ratio of the total amount of CO_2 emissions released by the ship over a year to the product of the ship's cargo transported and total distance over a year, and it is related to fuel consumption, sailing speed, load tonnage and mileage of voyage. The calculation formula of EEOI is Eq (1), which is given by the IMO [8].

$$\text{EEOI} = \frac{\text{total carbon emissions of the ship during ballast and laden voyages (g)}}{\text{amount of cargo transported} \times \text{total distance laden}} \tag{1}$$

Here, notice that the EEOI of a ship is also equal to the ratio of the total amount of CO_2 emissions released by the ship over a week to the product of the ship's cargo transported and total distance over a week because of the weekly service frequency. In addition, we assume that the ships owned by the liner company generate g tons of CO_2 when burning one ton of fuel, and let m_{ri} denote the volume of cargo load in the ship during leg i, $i \in I_r \cup I'_r$. Also, since we calculate the amount of CO_2 emissions in tons, but the amount of CO_2 emissions in the EEOI calculation formula is in grams, we need to multiply the amount of CO_2 emissions by 10^6 when calculating the EEOI value of each operating ship. Therefore, the average EEOI value of all ships deployed on all routes is $\sum_{r\in R}\frac{10^6(\varepsilon_r+7e_r\beta_r)g}{\sum_{i\in I_r} m_{ri}l_{ri}+\sum_{i\in I'_r} m_{ri}[l_{ri}\gamma_{ri}+l'_{ri}(1-\gamma_{ri})]}/\sum_{r\in R}\beta_r$.

Since this study aims to minimize both of the above objectives, i.e., the total weekly cost and the average EEOI value of all deployed ships on all routes, this study applies a typical way to solve the problem, which is the weighted sum method. We use λ as a weighting factor for the bi-objective programming which reveals the relative importance between the above two objective functions. Hence, the objective function of this problem is formulated as $\lambda\big[\sum_{r\in R}(o\beta_r + \sum_{i\in I'_r} q_r\gamma_{ri} + a_1\varepsilon_r + 7a_2e_r\beta_r)\big] + (1-\lambda)(\sum_{r\in R}\frac{10^6(\varepsilon_r+7e_r\beta_r)g}{\sum_{i\in I_r} m_{ri}l_{ri}+\sum_{i\in I'_r} m_{ri}[l_{ri}\gamma_{ri}+l'_{ri}(1-\gamma_{ri})]}/\sum_{r\in R}\beta_r)$.

3.3. Model formulation

Based on the above analysis of the objective function, this study formulates a nonlinear MIP model in this section. Before formulating the mathematical model for this problem, we list the notations used in this paper as follows.

Indices and sets:

R: set of all ship routes, $r \in R$.

I_r: set of all legs that do not cross Asian and European ports on ship route r, $i \in I_r$.

I'_r: set of all legs across Asian and European ports on ship route r, $i \in I'_r$.

V: set of all possible sailing speeds, $v \in V$, $V = \{\underline{v}, \underline{v}+0.1, \ldots, \overline{v}-0.1, \overline{v}\}$, where $\underline{v}$ and $\overline{v}$ represent the minimum and maximum speeds of ships on ship routes, respectively.

Z_+: set of all non-negative integers.

Parameters:

a_1, a_2: unit prices of fuels consumed by the main and auxiliary engines, respectively (USD/ton).

c_1, c_2, c_3: coefficients to calculate the unit fuel consumption for traveling per hour, which mainly depends on sailing speed and displacement (tons/hour).

d_{ri}: actual displacement of the ship during leg i on ship route r (tons).

e_r: amount of fuel consumed by the auxiliary engine of a ship deployed on ship route r per day (tons/day).

g : amount of CO_2 released by a ship when burning one ton of fuel (tons).

l_{ri}: length of the ith leg if $i \in I_r$ or length of the ith leg taking the Suez Canal route if $i \in I'_r$ on ship route r (n mile).

l'_{ri}: length of the ith ($i \in I'_r$) leg taking the Cape of Good Hope route on ship route r (n mile).

m_{ri}: cargo load in leg i, $i \in I_r \cup I'_r$, on ship route r (tons).

o: weekly operating cost of one ship deployed on ship routes (USD).

q_r: Suez Canal toll fee for a ship deployed on route r (USD/ship).

s_r: maximum number of ships that can be deployed on ship route r.

t_r: total duration a ship dwells at all ports of call on ship route r (hours).

λ: weighting factor for the bi-objective programming.

Variables:

α_{riv}: binary, equals 1 if and only if the speed of the ship sailing during leg i on ship route r is v; 0 otherwise.

γ_{ri}: binary, equals 1 if and only if the voyage option of leg i, $i \in I'_r$, on ship route r selects Suez Canal route; 0 if Cape of Good Hope route.

β_r: integer, number of ships deployed on ship route r.

ε_r: continuous, weekly fuel consumption of the main engine of all deployed ships on ship route r (tons).

Mathematical model

Based on the above definitions of parameters and variables, a nonlinear MIP model is formulated as follows.

[**M1**] $\text{Min } \lambda\left[\sum_{r\in R}(o\beta_r + \sum_{i\in I'_r} q_r\gamma_{ri} + a_1\varepsilon_r + 7a_2e_r\beta_r)\right]$

$$+(1-\lambda)\left(\sum_{r\in R}\frac{10^6(\varepsilon_r+7e_r\beta_r)g}{\sum_{i\in I_r} m_{ri}l_{ri}+\sum_{i\in I'_r} m_{ri}\left[l_{ri}\gamma_{ri}+l'_{ri}(1-\gamma_{ri})\right]}\Big/\sum_{r\in R}\beta_r\right) \quad (2)$$

subject to

$$1 \le \beta_r \le s_r \qquad \forall\ r \in R \quad (3)$$

$$\sum_{v\in V}\left(\sum_{i\in I_r}\frac{l_{ri}}{v}\alpha_{riv} + \sum_{i\in I'_r}\frac{l_{ri}\gamma_{ri}+l'_{ri}(1-\gamma_{ri})}{v}\alpha_{riv}\right) + t_r = 168\beta_r \qquad \forall\ r \in R \quad (4)$$

$$\varepsilon_r = \sum_{i\in I_r}\sum_{v\in V} c_1 v^{c_2}\alpha_{riv} d_{ri}{}^{c_3}\frac{l_{ri}}{v} + \sum_{i\in I_r'}\sum_{v\in V} c_1 v^{c_2}\alpha_{riv} d_{ri}{}^{c_3}\frac{l_{ri}\gamma_{ri}+l_{ri}'(1-\gamma_{ri})}{v} \quad \forall\ r\in R \tag{5}$$

$$\sum_{v\in V}\alpha_{riv} = 1 \qquad \forall\ r\in R, i\in I_r\cup I_r' \tag{6}$$

$$\alpha_{riv}\in\{0,1\} \qquad \forall\ r\in R, i\in I_r\cup I_r', v\in V \tag{7}$$

$$\beta_r\in Z_+ \qquad \forall\ r\in R \tag{8}$$

$$\gamma_{ri}\in\{0,1\} \qquad \forall\ r\in R, i\in I_r\cup I_r' \tag{9}$$

$$\varepsilon_r \geq 0. \qquad \forall\ r\in R \tag{10}$$

Objective (2) minimizes the weighted sum of two objectives considered in this study. Constraint (3) guarantees that at least one ship and at most s_r ships should be deployed on each route. Constraint (4) ensures that the total number of hours for a ship completing its travel on a route is the number of ships deployed on the route times 168, because all services follow the weekly arrival pattern, and one week has 168 hours. Constraint (5) calculates the weekly fuel consumption of the main engine of all deployed ships on ship route r. Constraint (6) ensures that sailing speeds of deployed ships during each leg on all ship routes satisfy the feasible speed range of ships. Constraints (7)–(10) state the ranges of the defined decision variables.

4. Algorithm design

It is challenging to solve the nonlinear model [M1], which contains multiple nonlinear parts, including objective function (2) and constraints (4) and (5). By reviewing several algorithms and their features in some existing fleet deployment studies, we find that specially tailored solution methods are usually designed for their models because these fleet deployment studies contain specific characteristics. For example, Zhen et al. [10] proposed a tailored dynamic linearization algorithm to solve a mixed-integer second-order cone programming model. In addition, considering specific characteristics of our problem, we find that nonlinear parts in model [M1] can be replaced by enumerating the possible values, and the model after the above transformation can be solved directly and effectively by Gurobi. Since the number of possible values of the nonlinear parts in model [M1] is small, this study designs an efficient exact algorithm based on the enumeration method to solve the model [M1]. Due to the efficiency and accuracy of the proposed algorithm, the proposed algorithm can quickly find the optimal solution of the model in a very short time.

Before introducing our algorithm, one transformation of constraint (4) is first introduced. Since sailing speed is discretized, the feasibility of constraint (4), which contains the equality symbol, might be affected. Hence, constraint (4) is replaced with constraint (11). Here, notice that the equality symbol in constraint (4) is replaced with the less than or equal to symbol in constraint (11).

$$\sum_{v\in V}\left(\sum_{i\in I_r}\frac{l_{ri}}{v}\alpha_{riv} + \sum_{i\in I_r'}\frac{l_{ri}\gamma_{ri}+l_{ri}'(1-\gamma_{ri})}{v}\alpha_{riv}\right) + t_r \leq 168\beta_r \qquad \forall\ r\in R. \tag{11}$$

As a result, the final version of model [M1] becomes the following:
[**M2**] objective (2) subject to constraints (3), (5)–(11).

Finally, we design the following exact algorithm, whose framework is introduced in Algorithm 1 to solve the model [M2]. The main difficulty in solving the model [M2] is the nonlinear part in objective (2). Two key techniques are applied to this nonlinear part. Specifically, the first one focuses on $\sum_{r\in R}\beta_r$ in the denominator. According to constraint (11), the number of ships deployed on route

r, denoted by $\beta_r^{\min}$, is at least $\beta_r^{\min} = \left\lceil (\sum_{i\in I_r} \frac{l_{ri}}{\overline{v}} + \sum_{i\in I_r'} \frac{\min(l_{ri}, l_{ri}')}{\overline{v}} + t_r)/168 \right\rceil$ (recall that $\overline{v}$ represents the maximum speed of ships on ship routes). Because constraint (3) guarantees that at most s_r ships could be deployed on route r, the value of $\sum_{r\in R} \beta_r$ ranges from $\sum_{r\in R} \beta_r^{\min}$ to $\sum_{r\in R} s_r$, which means we can directly enumerate the number of ships deployed on all ship routes. The other one is $\sum_{i\in I_r'} m_{ri}[l_{ri}\gamma_{ri} + l_{ri}'(1-\gamma_{ri})]$. In most cases, not all routes need to be reoptimized in terms of voyage option because these routes do not contain voyages across Asia and Europe. Even if all routes need to be reoptimized in terms of voyage option, the total number of voyage options on a single route is $|I_r'|$, which means there are $2^{|I_r'|}$ permutations of the values of γ_{ri} $(\forall r \in R, i \in I_r')$ for route r. Moreover, the value of $|I_r'|$ is either 0 or 2 because in real life, a liner route is either for a certain continent, or it only crosses Asian and European ports twice. Hence, the number of permutations is significantly small, and we can directly enumerate all permutations.

Algorithm 1. Framework of the proposed exact algorithm for solving model [M2]

$x \leftarrow \sum_{r\in R} \beta_r^{\min}$ // x records the number of ships deployed on all ship routes
$\mathrm{OBJ}^* \leftarrow \infty$ //OBJ^* records the incumbent objective function value of model [M2]
$(x, \gamma_{ri}, \forall r \in R, i \in I_r')^* \leftarrow$ null // $(x, \gamma_{ri}, \forall r \in R, i \in I_r')^*$ records the incumbent values of corresponding variables in [M2]
While $x \le \sum_{r\in R} s_r$ **do**
  Add constraint $\sum_{r\in R} \beta_r = x$ to model [M2]
  Obtain $2^{|I_1'|} \times 2^{|I_2'|} \times \cdots \times 2^{|I_{|R|}'|}$ permutations of $(\underbrace{\gamma_{1,1}, \gamma_{1,|I_1'|}}_{\text{route 1}}, \underbrace{\gamma_{2,1}, \gamma_{2,|I_2'|}}_{\text{route 2}}, \cdots, \underbrace{\gamma_{|R|,1}, \gamma_{|R|,|I_{|R|}'|}}_{\text{route } |R|})$
  $n \leftarrow 1$ //n is a counting number
  While $n \le 2^{|I_1'|} \times 2^{|I_2'|} \times \cdots \times 2^{|I_{|R|}'|}$ **do**
    Solve the updated model by Gurobi with given values $(\gamma_{ri}, \forall r \in R, i \in I_r')$ of the n^{th} permutation
    If model is feasible **then**
      If $\mathrm{OBJ} < \mathrm{OBJ}^*$ **then** //OBJ records the current objective function value obtained by Gurobi
        $(x, \gamma_{ri}, \forall r \in R, i \in I_r')^* \leftarrow (x, \gamma_{ri}, \forall r \in R, i \in I_r')$
        $\mathrm{OBJ}^* \leftarrow \mathrm{OBJ}$
      End if
    End if
  $n \leftarrow n + 1$
  End while
  Delete constraint $\sum_{r\in R} \beta_r = x$ from model [M2]
  $x \leftarrow x + 1$
End while
Solve model [M2] by Gurobi with given $(x, \gamma_{ri}, \forall r \in R, i \in I_r')^*$
Return the objective value and values of the variables

5. Computational experiments

In order to evaluate the efficiency of the proposed algorithm, we performed a large number of computational experiments on a PC (4 CPU cores, 1.6 GHz, Memory 8 GB). The mathematical models and algorithms proposed in this study are implemented in Gurobi 9.0.1 (Anaconda, Python). This section first summarizes the setting of our parameters in Section 5.1, validates the proposed algorithm in Section 5.2 and describes sensitivity analyses to seek managerial insights in Section 5.3.

5.1. Experimental setting

Sailing distance data, including l_{ri} and l'_{ri}, used in this study were obtained from the standard instances of LINER-LIB [33]. The value of the weekly fixed operating cost, i.e., o, is set to 180,000 USD, which is in line with the setting used in previous studies [11,34]. In real life, main and auxiliary engines of a ship may use the same type of fuel, such as liquefied natural gas (LNG). Therefore, this study assumes that main and auxiliary engines use the same type of fuel when calculating fuel costs of the main and auxiliary engines for the sake of simplicity in the computational experiments. Therefore, unit prices of fuels (i.e., a_1 and a_2) are set to 544.5 USD/ton because the average price of very low sulfur fuel oil (VLSFO) in global 20 ports in 2021 is 544.5 USD/ton [35]. For the sake of simplicity, a ship can only adjust its speeds by at least one knot in this study. The minimum and maximum values of sailing speed (i.e., $\underline{v}$ and $\overline{v}$) are set to 8 and 22 knots, respectively, which are also consistent with the settings used in related works [36,37]. The values of c_1, c_2 and c_3 are set to 0.00022, 2.5506 and 0.2072, respectively, which are consistent with the settings in related studies [9,36]. The value of the total duration, i.e., t_r, that a ship dwells at all ports of call on ship route r is randomly selected from $[24 \times (|I_r| + |I'_r|), 48 \times (|I_r| + |I'_r|)]$. The value of s_r (i.e., the maximum number of ships that can be deployed on ship route r) depends on the length of one cycle time, and it is set to 4 for regional ship routes or 10 for intercontinental shipping routes. The amount of CO_2 released by a ship when burning one ton of VLSFO, i.e., g, is set to 3.15 tons, which is in line with the realistic data from Lloyd's List [38]. Some parameters are generated by sampling from some normal distributions. Specifically, values of Suez Canal toll fee (i.e., q_r) of a ship on all routes are uniformly distributed over (400,000, 700,000) (USD/ship), which is in line with actual Suez Canal toll fees [39]. The average value of daily fuel consumption for the auxiliary engines (e_r) on all routes is set to 3 tons per day (normal distribution with standard deviation 0.5). The average value of cargo load (m_{ri}) on all legs is set to 180,000 tons (normal distribution with standard deviation 3000), and the value of actual displacement (d_{ri}) on all legs is set to $m_{ri} + 20{,}000$ tons.

5.2. Performance of the algorithm

We used the proposed exact algorithm to solve the model [M2] and conducted 11 sets of numerical experiments with different route compositions, which are summarized in Table 2. We first fixed $\lambda = 0.5$ and recorded computational results, including objective function value (OBJ_T), CPU running time (Time) and selected voyage option (Voyage option) in Table 3. Since the difference between the two objective function values in our model is very large, we normalize these two objective functions by dividing them by their respective maximum values. To obtain the maximum values, we set λ (i.e., the weighting factor for the bi-objective programming) to 0 and solve all computational experiments of

the model [M2] to get the maximum objective function value $\mathrm{OBJ}_1 = 15148529.7881$. Similarly, we set λ to 1 and solve all computational experiments of the model [M2] to get the maximum objective function value $\mathrm{OBJ}_2 = 0.3384$. From Table 3, we can see that the computing time increases with more routes, which is intuitive because more routes will bring more decision variables and constraints. Since the computing time of 6 routes is quick enough, case 10 is used for the following numerical experiments. The Suez Canal route was chosen in all experiments. This may be due to the fact that the Suez Canal route is more popular on trips because it saves more sailing time. Our algorithm has good performance because it can solve the numerical experiment with 7 ship routes and 32 legs in four minutes, which means our algorithm can be applied well to real problems and quickly provides optimal solutions for liner companies.

Table 2. Summary of seven routes.

Route ID	Port rotation (city)
1	Kaohsiung → Tokyo → Nagoya → Kaohsiung
2	General Santos City → Manila → Singapore → General Santos City
3	Hong Kong → Xiamen → Kaohsiung → Manila → Hong Kong
4	Kaohsiung → Keelung → Shanghai → Tanjung Pelepas → Jakarta → Kaohsiung
5	Laem Chabang → Colombo → Rotterdam → Hamburg → Singapore → Laem Chabang
6	Qingdao → Shanghai → Hong Kong → Singapore → Rotterdam → Singapore → Qingdao
7	Kaohsiung → Hong Kong → Singapore → Rotterdam → Singapore → Xiamen → Kaohsiung

Table 3. Computational results of the basic analysis.

Case ID	Route ID	OBJ_T	Time (s)	Voyage option
1	1, 5	0.53	1.20	Suez Canal
2	2, 6	0.61	1.51	Suez Canal
3	3, 5, 6	0.52	13.34	Suez Canal
4	4, 5, 6	0.56	14.38	Suez Canal
5	2, 4, 5, 6	0.69	16.76	Suez Canal
6	3, 4, 5, 6	0.70	18.54	Suez Canal
7	1, 3, 4, 5, 6	0.79	20.79	Suez Canal
8	2, 3, 4, 5, 6	0.84	24.40	Suez Canal
9	1, 2, 3, 5, 6	0.85	25.40	Suez Canal
10	1, 2, 3, 4, 5, 6	0.91	30.03	Suez Canal
11	1, 2, 3, 4, 5, 6, 7	0.94	222.25	Suez Canal

5.3. Sensitivity analyses

The impact of λ on the bi-objective programming is first described in this section. The value of λ ranged from 0 to 1. In Table 4, we show the normalized objective function value of model [M2] (OBJ_T), the total weekly cost value (OBJ_1), the average EEOI value of all deployed ships on all routes (OBJ_2), the total number of deployed ships ($\sum_{r\in R}\beta_r$), the selected voyage option (Voyage option) and the computing time (Time). It is obvious that OBJ_1 decreases with increasing λ, which is reasonable because a larger λ indicates a larger weight on OBJ_1. However, OBJ_2 stays the same at the beginning, then goes down and finally goes up. In addition, the total number of deployed ships decreases as the

value of λ increases. Finally, the change of the value of λ does not affect the voyage option, and the change of the value of λ has no obvious effect on the solution time. Therefore, with increasing λ (i.e., larger weight on the minimization of the total weekly cost), fewer ships are needed, which means that each deployed ship sails at a higher speed and releases more CO_2 (i.e., higher EEOI value). However, since the average EEOI value of all deployed ships on all routes is relatively small, the increase in the λ value in the early stage has no proportional effect on the second objective function value, i.e., OBJ_2.

Table 4. Impact of the weighting factor λ for the bi-objective programming.

λ	OBJ_T	OBJ_1 (USD)	OBJ_2 (g/ton/n mile)	$\sum_{r\in R}\beta_r$	Voyage option	Time (s)
0.0	0.9460	11349298.0951	0.3592	36	Suez Canal route	32.85
0.1	0.9514	11349298.0951	0.3592	36	Suez Canal route	31.37
0.2	0.9568	11349298.0951	0.3592	36	Suez Canal route	31.39
0.3	0.9622	11349298.0951	0.3592	36	Suez Canal route	33.15
0.4	0.9676	11349298.0951	0.3592	36	Suez Canal route	32.88
0.5	0.9572	11156852.8702	0.3536	35	Suez Canal route	32.13
0.6	0.9491	10967201.7128	0.3505	34	Suez Canal route	32.25
0.7	0.9434	10789871.1308	0.3517	33	Suez Canal route	31.02
0.8	0.9352	10619882.8389	0.3542	32	Suez Canal route	30.75
0.9	0.9311	10500058.7455	0.3737	31	Suez Canal route	31.25
1.0	0.9201	10442771.8214	0.3796	30	Suez Canal route	28.62

Notes: 1) "OBJ_T," "OBJ_1," "OBJ_2" and "$\sum_{r\in R}\beta_r$" represent the normalized OBJ value of model [M2], total weekly cost value, average EEOI value of all deployed ships on all routes and the total number of deployed ships, respectively. 2) "Voyage option" represents the voyage selection of deployed ships across Asian and European ports, i.e., Suez Canal route or Cape of Good Hope route. 3) "Time" represents CPU running time (s).

Table 5. Impact of unit price of fuel on the operation decisions.

a (USD/ton)	OBJ_T	OBJ_1 (USD)	OBJ_2 (g/ton/n mile)	$\sum_{r\in R}\beta_r$	Voyage option
200.00	0.8602	9,285,432.4798	0.3505	34	Suez Canal route
300.00	0.8860	9,773,609.3254	0.3505	34	Suez Canal route
400.00	0.9118	10,261,786.1709	0.3505	34	Suez Canal route
500.00	0.9376	10,749,963.0165	0.3505	34	Suez Canal route
600.00	0.9634	11,238,139.8621	0.3505	34	Suez Canal route
700.00	0.9892	11,726,316.7077	0.3505	34	Suez Canal route
800.00	1.0150	12,214,493.5533	0.3505	34	Suez Canal route
900.00	1.0408	12,702,670.3988	0.3505	34	Suez Canal route
1000.00	1.0666	13,190,847.2444	0.3505	34	Suez Canal route
1100.00	1.0924	13,679,024.0900	0.3505	34	Suez Canal route
1200.00	1.1183	14,167,200.9356	0.3505	34	Suez Canal route

Notes: ① "OBJ_T," "OBJ_1," "OBJ_2," and "$\sum_{r\in R}\beta_r$" represent the normalized OBJ value of model [M2], total weekly cost value, average EEOI value of all deployed ships on all routes and the total number of deployed ships, respectively. ② "Voyage option" represents the voyage selection of deployed ships across Asian and European ports, i.e., Suez Canal route or Cape of Good Hope route.

We next studied the impact of unit price of fuel on the operation decisions. According to S&B [35], the lowest and highest prices of VLSFO in global 20 ports from January 01, 2020, to July 14, 2022, were 211.25 USD/ton, and 1120.50 USD/ton, respectively. Hence, we set the value of a from 200 to 1200 USD/ton to investigate its influence. Relevant results, including $\mathrm{OBJ_T}$, $\mathrm{OBJ_1}$, $\mathrm{OBJ_2}$, $\sum_{r\in R}\beta_r$ and Voyage option, are presented in Table 5. In order to make the result more intuitive, we also give Figure 2, whose abscissa is the fuel price, and the primary and secondary ordinate axes are $\mathrm{OBJ_1}$ and $\mathrm{OBJ_2}$, respectively. When the unit price of fuel increases, both $\mathrm{OBJ_T}$ and $\mathrm{OBJ_1}$ increase because the weekly fuel cost increases, but $\mathrm{OBJ_2}$ is not influenced by fuel price. In addition, changes in the fuel price do not affect fleet deployment and voyage option decisions. The above observations are reasonable because changes in the unit price of fuel do not cause changes in fleet deployment strategies and sailing speeds, resulting in no changes in $\mathrm{CO_2}$ emissions and no changes in the value of the second objective function. However, the continuous increase in the unit price of fuel leads to an increase in the weekly fuel consumption cost, which eventually leads to an increase in the value of the first objective function.

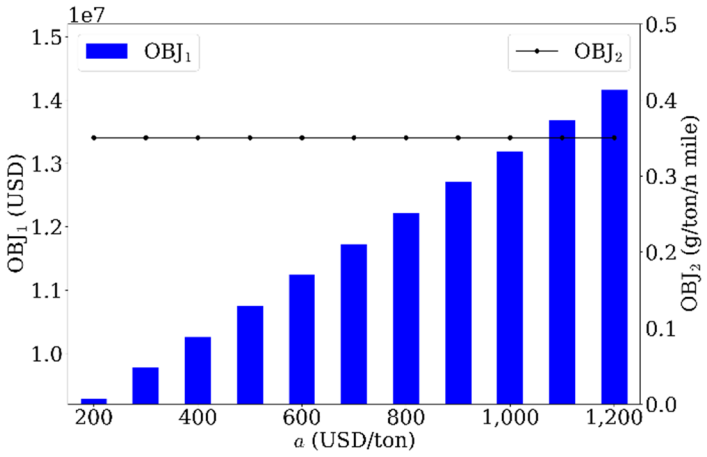

Figure 2. Comparison of $\mathrm{OBJ_1}$ and $\mathrm{OBJ_2}$ values under different values of a.

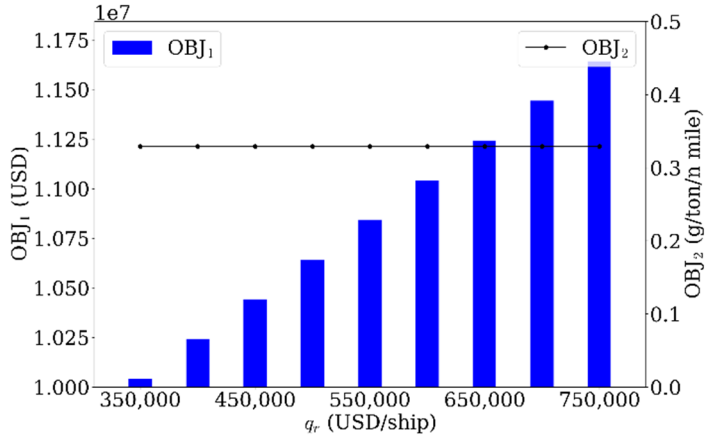

Figure 3. Comparison of $\mathrm{OBJ_1}$ and $\mathrm{OBJ_2}$ values under different values of q_r.

Next, we discuss the impact of Suez Canal toll fee per ship on the operation decisions. According to HKTDC [39], Suez Canal toll fees for a ship range from 400,000 to 700,000 USD. Hence, we set

the Suez Canal toll fee for a ship from 350,000 to 750,000 USD/ship to investigate its influence. Relevant results, including $\mathrm{OBJ_T}$, $\mathrm{OBJ_1}$, $\mathrm{OBJ_2}$, $\sum_{r\in R}\beta_r$ and Voyage option, are given in Table 6. In order to make the result more intuitive, we also give Figure 3, whose abscissa is the Suez Canal toll fee per ship, and the primary and secondary ordinate axes are $\mathrm{OBJ_1}$ and $\mathrm{OBJ_2}$, respectively. When the Suez Canal toll fee per ship increases, both $\mathrm{OBJ_T}$ and $\mathrm{OBJ_1}$ increase, but $\mathrm{OBJ_2}$ does not change with increasing q_r. In addition, changes in the Suez Canal toll fee per ship do not affect fleet deployment and voyage option decisions, which further makes the EEOI of each ship unchanged, as the ship's $\mathrm{CO_2}$ emissions and mileage do not change. The above observations are reasonable because the weekly Suez Canal toll fee is small compared to the weekly fuel consumption and operating costs of deployed ships. Therefore, the increase in the Suez Canal toll fee per ship does not lead to changes in fleet deployment, sailing speeds and voyage planning.

Table 6. Impact of Suez Canal toll fee per ship on the operation decisions.

q_r (USD/ship)	$\mathrm{OBJ_T}$	$\mathrm{OBJ_1}$ (USD)	$\mathrm{OBJ_2}$ (g/ton/n mile)	$\sum_{r\in R}\beta_r$	Voyage option
350,000.00	0.8775	10,042,966.9490	0.3289	34	Suez Canal route
400,000.00	0.8881	10,242,966.9490	0.3289	34	Suez Canal route
450,000.00	0.8986	10,442,966.9490	0.3289	34	Suez Canal route
500,000.00	0.9092	10,642,966.9490	0.3289	34	Suez Canal route
550,000.00	0.9198	10,842,966.9490	0.3289	34	Suez Canal route
600,000.00	0.9304	11,042,966.9490	0.3289	34	Suez Canal route
650,000.00	0.9409	11,242,966.9490	0.3289	34	Suez Canal route
700,000.00	0.9515	11,442,966.9490	0.3289	34	Suez Canal route
750,000.00	0.9621	11,642,966.9490	0.3289	34	Suez Canal route

Notes: 1) "$\mathrm{OBJ_T}$," "$\mathrm{OBJ_1}$," "$\mathrm{OBJ_2}$," and "$\sum_{r\in R}\beta_r$" represent the normalized OBJ value of model [M2], total weekly cost value, average EEOI value of all deployed ships on all routes and the total number of deployed ships, respectively. 2) "Voyage option" represents the voyage selection of deployed ships across Asian and European ports, i.e., Suez Canal route or Cape of Good Hope route.

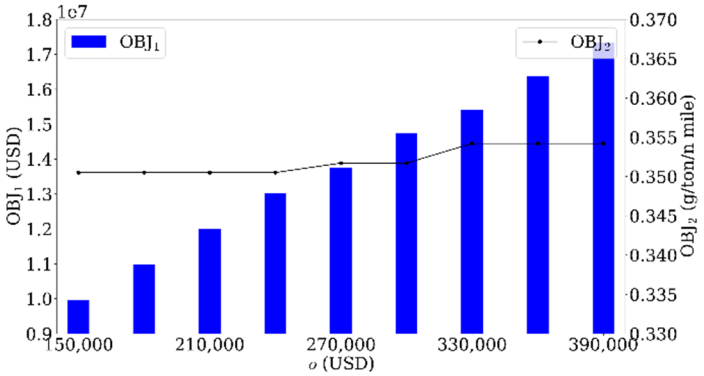

Figure 4. Comparison of $\mathrm{OBJ_1}$ and $\mathrm{OBJ_2}$ values under different values of o.

In the basic experiment, the value of the weekly fixed operating cost (o) was set to 180,000 USD. However, weekly operating costs may double several times due to outbreaks and other reasons. To analyze the impact of weekly fixed operating cost on the operation decisions, we set the value of o from 150,000 USD to 390,000 USD. Relevant results, including $\mathrm{OBJ_T}$, $\mathrm{OBJ_1}$, $\mathrm{OBJ_2}$ $\sum_{r\in R}\beta_r$ and

Voyage option are given in Table 7. In order to make the result more intuitive, we also give Figure 4, whose abscissa is the weekly operating cost, and the primary and secondary ordinate axes are OBJ_1 and OBJ_2, respectively. When the weekly operating cost increases, all of OBJ_T, OBJ_1 and OBJ_2 increase, but OBJ_2 remains unchanged in the three intervals [150,000, 240,000], [270,000, 300,000] and [330,000, 390,000]. In addition, changes in the weekly fixed operating cost directly influence fleet deployment but do not affect voyage option decision. The above observations are reasonable because the weekly fixed operating cost accounts for a large proportion of the total weekly cost. The continuous increase in the weekly fixed operating cost causes liner companies to reduce the number of deployed ships, which causes ships to sail at higher speeds to maintain the weekly arrival pattern. Moreover, high speeds of deployed ships cause more CO_2 emissions.

Table 7. Impact of weekly fixed operating cost on the operation decisions of ship fleets.

o (USD)	OBJ_T	OBJ_1 (USD)	OBJ_2 (g/ton/n mile)	$\sum_{r\in R}\beta_r$	Voyage option
150,000.00	0.8952	9,947,201.7128	0.3505	34	Suez Canal route
180,000.00	0.9491	10,967,201.7128	0.3505	34	Suez Canal route
210,000.00	1.0030	11,987,201.7128	0.3505	34	Suez Canal route
240,000.00	1.0569	13,007,201.7128	0.3505	34	Suez Canal route
270,000.00	1.0980	13,759,871.1308	0.3517	33	Suez Canal route
300,000.00	1.1503	14,749,871.1308	0.3517	33	Suez Canal route
330,000.00	1.1884	15,419,882.8389	0.3542	32	Suez Canal route
360,000.00	1.2392	16,379,882.8389	0.3542	32	Suez Canal route
390,000.00	1.2899	17,339,882.8389	0.3542	32	Suez Canal route

Notes: 1) "OBJ_T," "OBJ_1," "OBJ_2" and "$\sum_{r\in R}\beta_r$" represent the normalized OBJ value of model [M2], total weekly cost value, average EEOI value of all deployed ships on all routes and the total number of deployed ships, respectively. 2) "Voyage option" represents the voyage selection of deployed ships across Asian and European ports, i.e., Suez Canal route or Cape of Good Hope route.

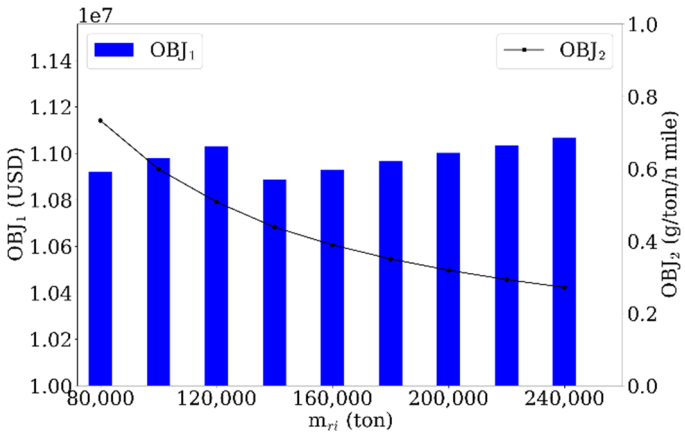

Figure 5. Comparison of OBJ_1 and OBJ_2 values under different values of m_{ri}.

Finally, we investigated the impact of cargo load on the operation decisions. In the basic experiment, the average value of cargo load (m_{ri}) was set to 180,000 tons (normal distribution with standard deviation 3000). Hence, we set the average value of cargo load in each leg from 80,000 to 240,000 (normal distribution with standard deviation 3000) to investigate its influence. Relevant results,

including $\mathrm{OBJ_T}$, $\mathrm{OBJ_1}$, $\mathrm{OBJ_2}$, $\sum_{r\in R}\beta_r$ and Voyage option, are given in Table 8. In order to make the result more intuitive, we also give Figure 5, whose abscissa is the cargo load in each leg, and the primary and secondary ordinate axes are $\mathrm{OBJ_1}$ and $\mathrm{OBJ_2}$, respectively. When the cargo load in each leg increases, $\mathrm{OBJ_T}$ and $\mathrm{OBJ_1}$ increase, but $\mathrm{OBJ_2}$ and the number of deployed ships decrease. However, voyage option decision is not influenced by changes in the cargo load. The above observations are reasonable because, with the increase in the cargo load, the product of the ship's cargo transported and the total distance over a week becomes larger. Although the ship sails at a higher speed due to the fewer deployed ships, the increase in the product of the ship's cargo transported and total distance over a week has a more significant impact on the expected EEOI value of all deployed ships than the increase in sailing speeds. Therefore, the average EEOI value of all deployed ships increases significantly with the increase in cargo load.

Table 8. Impact of cargo load in each voyage on the operation decisions.

m_{ri} (ton)	$\mathrm{OBJ_T}$	$\mathrm{OBJ_1}$ (USD)	$\mathrm{OBJ_2}$ (g/ton/n mile)	$\sum_{r\in R}\beta_r$	Voyage option
80,000.00	1.3500	10,919,422.4394	0.7334	35	Suez Canal route
100,000.00	1.2115	10,978,604.3255	0.5990	35	Suez Canal route
120,000.00	1.1185	11,030,417.9005	0.5082	35	Suez Canal route
140,000.00	1.0375	10,887,008.8904	0.4385	34	Suez Canal route
160,000.00	0.9879	10,928,874.5838	0.3892	34	Suez Canal route
180,000.00	0.9491	10,967,201.7128	0.3505	34	Suez Canal route
200,000.00	0.9180	11,002,602.1327	0.3192	34	Suez Canal route
220,000.00	0.8925	11,035,537.2494	0.2934	34	Suez Canal route
240,000.00	0.8713	11,066,364.2305	0.2717	34	Suez Canal route

Notes: 1) "$\mathrm{OBJ_T}$," "$\mathrm{OBJ_1}$," "$\mathrm{OBJ_2}$" and "$\sum_{r\in R}\beta_r$" represent the normalized OBJ value of model [M2], total weekly cost value, average EEOI value of all deployed ships on all routes and the total number of deployed ships, respectively. 2) "Voyage option" represents the voyage selection of deployed ships across Asian and European ports, i.e., Suez Canal route or Cape of Good Hope route.

In summary, this study investigated the impact of λ on the bi-objective programming and the impacts of unit price of fuel, Suez Canal toll fee per ship, weekly fixed operating cost and cargo load on the operation decisions. Specifically, with increasing λ (larger weight on the minimization of the total weekly cost), fewer ships are needed, which means that each deployed ship sails at a higher speed and releases more $\mathrm{CO_2}$ (i.e., higher EEOI value). In addition, the increase in the λ value in the early stage has no significant effect on the second objective function value. For the impact of unit price of fuel on the operation decisions, if changes in the unit price of fuel do not cause changes in fleet deployment strategies and sailing speeds, the amount of $\mathrm{CO_2}$ emissions and the expected EEOI value of all deployed ships will stay the same. However, the continuous increase in the unit price of fuel leads to an increase in the weekly fuel consumption cost, which eventually leads to an increase in the total weekly cost. For the impact of Suez Canal toll fee per ship on the operation decisions, since the weekly Suez Canal toll fee is less than the weekly fuel consumption and operating costs of deployed ships, the increase in the Suez Canal toll fee per ship does not lead to changes in fleet deployment, sailing speeds and voyage options. However, for the impact of the weekly fixed operating cost on the operation decisions, since the weekly fixed operating cost accounts for a large proportion of the total weekly cost, the continuous increase in the weekly fixed operating cost causes liner companies to

reduce the number of deployed ships and causes ships to sail at higher speeds. Finally, for the impact of cargo load on the operation decisions, with the increase in the cargo load, the increase in the product of the ship's cargo transported and total distance over a week has a more significant impact on the expected EEOI value of all deployed ships than the increase in sailing speeds. Therefore, the average EEOI value of all deployed ships increases significantly with the increase in cargo load.

6. Conclusions

The existing literature lacks research on the integrated optimization problem of fleet deployment, voyage planning and speed optimization with consideration of the influences of sailing speed, displacement and voyage option on fuel consumption. To fill this research gap, this study formulates a nonlinear MIP model capturing all these elements and designs a tailored exact algorithm for the model. Contributions of this paper are summarized from the following three aspects.

1) A nonlinear MIP model is proposed for this problem with the aim of minimizing both the total weekly cost and the average EEOI value of all deployed ships on all routes by determining the optimal sailing speed during each leg, the voyage option between the Suez Canal route and Cape of Good Hope route and the number of ships deployed on each ship route. 2) To deal with the challenge of solving a nonlinear MIP model, a tailored exact algorithm is proposed by considering specific characteristics of our problem. Efficiency of the proposed algorithm for computational instances of different sizes is verified. 3) Sensitivity analyses with crucial parameters, including the weighting factor, unit price of fuel, Suez Canal toll fee per ship, weekly fixed operating cost and cargo load in each leg, are carried out to show the influences of these factors on the results to obtain managerial insights. For example, with increasing λ (i.e., larger weight on the minimization of the total weekly cost), fewer ships are needed, which means that each deployed ship needs to sail at a higher speed and releases more CO_2 (i.e., higher EEOI value).

In the future, uncertain shipping transportation in demand can be incorporated in the problem because shipping transportation demands change dramatically from time to time, and uncertainty affects the performance of transportation systems under different conditions [40–43]. In addition, container terminal planning [44–47] can be integrated into the fleet deployment problem. Additionally, fleet deployment with the consideration of subsidy design [48,49] can also be studied. Finally, several new techniques can be incorporated into the fleet deployment problem, such as computer vision algorithms [50], deep learning [51], blockchain technology [52], autonomous driving [53], cooling system management [54,55], combined prediction and optimization [56,57] and supply chain management [58].

Conflict of interest

The authors declare there are no conflict of interest.

References

1. *United States Environmental Protection Agency (USEPA)*, Sources of greenhouse gas emissions, 2022. Available from: https://www.epa.gov/ghgemissions/sources-greenhouse-gas-emissions.

2. *S. S. Young (SSY)*, Smoke and mirrors: new decarbonisation regulations meet rising emissions, 2022. Available from: https://www.ssyonline.com/our-blog/posts/2022/january-2022/smoke-and-mirrors-new-decarbonisation-regulations-meet-rising-emissions/.
3. *International Maritime Organization (IMO)*, Third IMO greenhouse gas study, 2014. Available from: https://gmn.imo.org/wp-content/uploads/2017/05/GHG3-Executive-Summary-and-Report_web.pdf.
4. *United Nations (UN)*, Paris agreement, 2015. Available from: https://unfccc.int/sites/default/files/english_paris_agreement.pdf.
5. *International Maritime Organization (IMO)*, Initial IMO GHG strategy, 2018. Available from: https://www.imo.org/en/MediaCentre/HotTopics/Pages/Reducing-greenhouse-gas-emissions-from-ships.aspx.
6. *Lloyd's List*, Shipping emissions rise 4.9% in 2021, 2022. Available from: https://lloydslist.maritimeintelligence.informa.com/LL1139627/Shipping-emissions-rise-49-in-2021.
7. *International Maritime Organization (IMO)*, Guidelines for voluntary use of the ship energy efficiency operational indicator (EEOI), 2009. Available from: https://gmn.imo.org/wp-content/uploads/2017/05/Circ-684-EEOI-Guidelines.pdf.
8. *International Maritime Organization (IMO)*, Report of the marine environment protection committee on its sixty-second session, 2011. Available from: https://euroshore.com/sites/euroshore.com/files/downloads/mepc%2062-24.pdf.
9. Q. Meng, Y. Du, Y. Wang, Shipping log data based container ship fuel efficiency modeling, *Transport. Res. Part B Methodol.*, **83** (2016), 207–229. https://doi.org/10.1016/j.trb.2015.11.007
10. L. Zhen, S. Wang, G. Laporte, Y. Hu, Integrated planning of ship deployment, service schedule and container routing, *Comput. Oper. Res.*, **104** (2019), 304–318. https://doi.org/10.1016/j.cor.2018.12.022
11. L. Zhen, Y. Hu, S. Wang, G. Laporte, Y. Wu, Fleet deployment and demand fulfillment for container shipping liners, *Transp. Res. Part B Methodol.*, **120** (2019), 15–32. https://doi.org/10.1016/j.trb.2018.11.011
12. Q. Meng, S. Wang, H. Andersson, K. Thun, Containership routing and scheduling in liner shipping: overview and future research directions, *Transp. Sci.*, **48** (2014), 265–280. https://doi.org/10.1287/trsc.2013.0461
13. S. Wang, Q. Meng, Container liner fleet deployment: A systematic overview, *Transport. Res. Part C Emerging Technol.*, **77** (2017), 389–404. https://doi.org/10.1016/j.trc.2017.02.010
14. M. Christiansen, E. Hellsten, D. Pisinger, D. Sacramento, C. Vilhelmsen, Liner shipping network design, *Eur. J. Opre. Res.*, **286** (2020), 1–20. https://doi.org/10.1016/j.ejor.2019.09.057
15. X. Lai, L. Wu, K. Wang, F. Wang, Robust ship fleet deployment with shipping revenue management, *Transp. Res. Part B Methodol.*, **161** (2022), 169–196. https://doi.org/10.1016/j.trb.2022.05.005
16. V. Zisi, H. N Psaraftis, T. Zis, The impact of the 2020 global sulfur cap on maritime CO_2 emissions, *Marit. Bus. Rev.*, **6** (2021), 339–357. https://doi.org/10.1108/MABR-12-2020-0069
17. M. Zhu, K. F. Yuen, J. W. Ge, K. X. Li, Impact of maritime emissions trading system on fleet deployment and mitigation of CO2 emission, *Transp. Res. Part D Transp. Environ.*, **62** (2018), 474–488. https://doi.org/10.1016/j.trd.2018.03.016

18. S. Wang, D. Zhuge, L. Zhen, C. Y. Lee, Liner shipping service planning under sulfur emission regulations, *Transp. Sci.*, **55** (2021), 491–509. https://doi.org/10.1287/trsc.2020.1010
19. J. Pasha, M. A. Dulebenets, A. M. Fathollahi-Fard, G. Tian, Y. Y. Lau, P. Singh, et al., An integrated optimization method for tactical-level planning in liner shipping with heterogeneous ship fleet and environmental considerations, *Adv. Eng. Inf.*, **48** (2021), 101299. https://doi.org/10.1016/j.aei.2021.101299
20. Y. Zhao, J. Ye, J. Zhou, Container fleet renewal considering multiple sulfur reduction technologies and uncertain markets amidst COVID-19, *J. Clean. Prod.*, **317** (2021), 128361. https://doi.org/10.1016/j.jclepro.2021.128361
21. J. Chen, J. Ye, A. Liu, Y. Fei, Z. Wan, X. Huang, Robust optimization of liner shipping alliance fleet scheduling with consideration of sulfur emission restrictions and slot exchange, *Ann. Oper. Res.*, **2022** (2022), 1–31. https://doi.org/10.1007/s10479-022-04590-x
22. Y. Zhao, Y. Fan, K. Fagerholt, J. Zhou, Reducing sulfur and nitrogen emissions in shipping economically, *Transp. Res. Part D Transp. Environ.*, **90** (2021), 102641. https://doi.org/10.1016/j.trd.2020.102641
23. N. Acomi, O. C. Acomi, Improving the voyage energy efficiency by using EEOI, *Procedia-Social Behav. Sci.*, **138** (2014), 531–536. https://doi.org/10.1016/j.sbspro.2014.07.234
24. Y. Hou, K. Kang, X. Liang, Vessel speed optimization for minimum EEOI in ice zone considering uncertainty, *Ocean. Eng.*, **188** (2019), 106240. https://doi.org/10.1016/j.oceaneng.2019.106240
25. C. Sun, H. Wang, C. Liu, Y. Zhao, Dynamic prediction and optimization of energy efficiency operational index (EEOI) for an operating ship in varying environments, *J. Mar. Sci. Eng.*, **7** (2019), 402. https://doi.org/10.3390/jmse7110402
26. M. Ichsan, M. F. Pradana, B. Noche, Estimation and optimization of the voyage energy efficiency operational indicator (EEOI) on Indonesian sea tollway corridors, in *IOP Conference Series: Materials Science and Engineering.*, **673** (2019), 012024. https://doi.org/10.1088/1757-899X/673/1/012024
27. K. Prill, C. Behrendt, M. Szczepanek, I. Michalska-Pożoga, A new method of determining energy efficiency operational indicator for specialized ships, *Energies*, **13** (2020), 1082. https://doi.org/10.3390/en13051082
28. Y. Hou, Y. Xiong, Y. Zhang, X. Liang, L. Su, Vessel energy efficiency uncertainty optimization analysis in ice zone considering interval parameters, *Ocean Eng.*, **232** (2021), 109114. https://doi.org/10.1016/j.oceaneng.2021.109114
29. J. Zhou, Y. Zhao, J. Liang, Multiobjective route selection based on LASSO regression: when will the Suez Canal lose its importance? *Math. Prob. Eng.*, **2021** (2021), 6613332. https://doi.org/10.1155/2021/6613332
30. Y. Zhao, Y. Fan, J. Zhou, H. Kuang, Bi-objective optimization of vessel speed and route for sustainable coastal shipping under the regulations of emission control areas, *Sustainability*, **11** (2019), 6281. https://doi.org/10.3390/su11226281
31. S. Wang, Q. Meng, Sailing speed optimization for container ships in a liner shipping network, *Transport. Transp. Res. Part E Logist. Transp. Rev.*, **48** (2012), 701–714. https://doi.org/10.1016/j.tre.2011.12.003
32. Y. Zhao, J. Zhou, Y. Fan, H. Kuang, Sailing speed optimization model for slow steaming considering loss aversion mechanism, *J. Adv. Transp.*, **2020** (2020), 2157945. https://doi.org/10.1155/2020/2157945

33. B. D. Brouer, J. F. Alvarez, C. E. M. Plum, D. Pisinger, M. M. Sigurd, A base integer programming model and benchmark suite for liner-shipping network design, *Transp. Sci*., **48** (2013), 281–312. https://doi.org/10.1287/trsc.2013.0471
34. A. Alharbi, S. Wang, P. Davy, Schedule design for sustainable container supply chain networks with port time windows, *Adv. Eng. Inf*., **29** (2015), 322–331. https://doi.org/10.1016/j.aei.2014.12.001
35. *Ship and Bunker (S&B)*, World bunker prices, 2022. Available from: https://shipandbunker.com/prices/av/global/av-g20-global-20-ports-average.
36. Y. Wang, Q. Meng, Y. Du, Liner container seasonal shipping revenue management. *Transp. Res. Part B Methodol.*, **82** (2015), 141–161. https://doi.org/10.1016/j.trb.2015.10.003
37. L. Zhen, Y. Wu, S. Wang, G. Laporte, Green technology adoption for fleet deployment in a shipping network, *Transp. Res. Part B Methodol.*, **139** (2020), 388–410. https://doi.org/10.1016/j.trb.2020.06.004
38. *Lloyd's List*, Shipowners focus on 2030 carbon cut target, 2021. Available from: https://lloydslist.maritimeintelligence.informa.com/LL1136881/Shipowners-focus-on-2030-carbon-cut-target.
39. *HKTDC*, Egypt: Suez Canal temporarily slashes fees for Asia-bound shipping, 2020. Available from: https://research.hktdc.com/en/article/NDI2MDE2NTg2.
40. L. Zhen, Y. Wu, S. Wang, Y. Hu, W. Yi, Capacitated closed-loop supply chain network design under uncertainty, *Adv. Eng. Inf*., **38** (2018), 306–315. https://doi.org/10.1016/j.aei.2018.07.007
41. D. Huang, S. Wang, A two-stage stochastic programming model of coordinated electric bus charging scheduling for a hybrid charging scheme, *Multimodal Transp*., **1** (2022), 100006. https://doi.org/10.1016/j.multra.2022.100006
42. W. Wang, Y. Wu, Is uncertainty always bad for the performance of transportation systems? *Commun. Transp. Res*., **1** (2021), 100021. https://doi.org/10.1016/j.commtr.2021.100021
43. J. Zhang, D. Z. Long, R. Wang, C. Xie, Impact of penalty cost on customers' booking decisions, *Prod. Oper. Manage*., **30** (2021), 1603–1614. https://doi.org/10.1111/poms.13297
44. Y. Ding, K. Chen, D. Xu, Q. Zhang, Dynamic pricing research for container terminal handling charge, *Marit. Policy Manage*., **48** (2021) 512–529. https://doi.org/10.1080/03088839.2020.1790051
45. M. Kim, Y. Jeong, I. Moon, Efficient stowage plan with loading and unloading operations for shipping liners using foldable containers and shift cost-sharing, *Marit. Policy Manage*., **48** (2021), 877–894. https://doi.org/10.1080/03088839.2020.1821109
46. X. Song, J. G. Jin, H. Hu, Planning shuttle vessel operations in large container terminals based on waterside congestion cases, *Marit. Policy Manage*., **48** (2021), 988–1009. https://doi.org/10.1080/03088839.2020.1719443
47. L. Wu, Y. Adulyasak, J. F. Cordeau, S. Wang, Vessel service planning in seaports, *Oper. Res*., **70** (2022), 2032–2053. https://doi.org/10.1287/opre.2021.2228
48. W. Yi, S. Wu, L. Zhen, G. Chawynski, Bi-level programming subsidy design for promoting sustainable prefabricated product logistics, *Cleaner Logist. Supply Chain*, **1** (2021), 100005. https://doi.org/10.1016/j.clscn.2021.100005
49. W. Yi, L. Zhen, Y. Jin, Stackelberg game analysis of government subsidy on sustainable off-site construction and low-carbon logistics, *Cleaner Logist. Supply Chain*, **2** (2021), 100013. https://doi.org/10.1016/j.clscn.2021.100013

50. W. Yi, H. Wang, Y. Jin, J. Cao, Integrated computer vision algorithms and drone scheduling, *Commun. Transp. Res*., **1** (2021), 100002. https://doi.org/10.1016/j.commtr.2021.100002
51. W. Zhu, J. Wu, T. Fu, J. Wang, J. Zhang, Q. Shangguan, Dynamic prediction of traffic incident duration on urban expressways: a deep learning approach based on LSTM and MLP, *J. Intell. Connected. Veh*., **4** (2021), 80–91. https://doi.org/10.1108/JICV-03-2021-0004
52. E. Hirata, M. Lambrou, D. Watanabe, Blockchain technology in supply chain management: insights from machine learning algorithms, *Marit. Bus. Rev*., **6** (2021), 114–128. https://doi.org/10.1108/MABR-07-2020-0043
53. Y. Li, S. E. Li, X. Jia, S. Zeng, Y. Wang, FPGA accelerated model predictive control for autonomous driving, *J. Intell. Connected. Veh*., **5** (2022), 63–71. https://doi.org/10.1108/JICV-03-2021-0002
54. A. P. C. Chan, W. Yi, F. K. Wong, Evaluating the effectiveness and practicality of a cooling vest across four industries in Hong Kong, *Facilities*, **34** (2016), 511–534. https://doi.org/10.1108/F-12-2014-0104
55. W. Yi, Y. Zhao, A. P. C. Chan, Evaluating the effectiveness of cooling vest in a hot and humid environment, *Ann. Work Exposures Health*, **61** (2017), 481–494. https://doi.org/10.1093/annweh/wxx007
56. S. Wang, R. Yan, A global method from predictive to prescriptive analytics considering prediction error for "Predict, then optimize" with an example of low-carbon logistics, *Cleaner Logist. Supply Chain*, **4** (2022) 100062. https://doi.org/10.1016/j.clscn.2022.100062
57. R. Yan, S. Wang, Integrating prediction with optimization: models and applications in transportation management, *Multimodal Transp*., **1** (2022), 100018. https://doi.org/10.1016/j.multra.2022.100018
58. L. Zhang, L. Guan, D. Z Long, H. Shen, H. Tang, Who is better off by selling extended warranties in the supply chain: the manufacturer, the retailer, or both? *Ann. Oper. Res*., **2020** (2020). https://doi.org/10.1007/s10479-020-03728-z

AIMS Press